Measurements of the Flory−Huggins Interaction Parameter for Polystyrene−Poly(4-vinylpyridine) Blends

C. J. Clarke*,† and A. Eisenberg

Department of Chemistry, McGill University, 801 Sherbrooke Street West, Montreal, P.Q. H3A 2K6, Canada

J. La Scala, M. H. Rafailovich, J. Sokolov, Z. Li, and S. Qu

Department of Materials Science and Engineering, State University of New York at Stony Brook, Stony Brook, New York 11794

D. Nguyen

Brookhaven National Laboratory, Upton, New York 11973

S. A. Schwarz and Y. Strzhemechny

Dept. of Physics, Queens College, Flushing, New York 11367

B. B. Sauer

E. I. Dupont, Nemours and Co. Inc., Experimental Station, Wilmington, Delaware 19880

Received July 30, 1996; Revised Manuscript Received April 2, 1997[⊗]

ABSTRACT: We have measured the Flory−Huggins interaction parameter (χ) for blends of polystyrene (PS) and poly(4-vinylpyridine) (P4VP) by three different methods. First, we measured the micelle spacings in microphase-separated films of PS−P4VP diblock copolymers by secondary ion mass spectrometry and atomic force microscopy. Second, we measured the contact angle of droplets of homopolymer PS on P4VP homopolymer film. Finally we determined the interfacial width between homopolymer layers of dPS and P4VP by neutron reflectometry. From each of these experiments χ was calculated using mean field theory in the strong segregation limit. These values of χ are much larger than those of other nonionic polymer pairs. We discuss the importance of this findings.

Introduction

The study of the microstructures formed by immiscible polymer blends and block copolymers has attracted a large amount of theoretical and experimental interest in recent years (see for example refs 1−5). These systems have properties which are not found in simple melts of the individual components and which depend crucially on the compatibility of the polymers. For most polymer pairs there is a small unfavorable interaction between monomers. This usually leads to phase separation because of the large number of monomers per macromolecule, so that the entropy of mixing becomes small. The important quantity is χN where N is the degree of polymerization and χ is the Flory−Huggins interaction parameter.

The thermodynamic principles which determine the microstructures are well understood and are typically described in terms of one of two regimes: the weak segregation limit,[1] which is valid near the critical point of microphase separation, and the strong segregation limit, which is valid when there are well-separated domains with narrow interfaces between them ($\chi N > 1$, $\chi < 1$).[2] Recently Nyrkova et al.[3] have theoretically predicted a third regime, "super-strong segregation" for very large χ. While many systems are well described by the weak and strong segregation regimes, there have been no experimental observations of the super strong segregation regime. Large values of χ have been observed in ionomers, where single ionic groups can cause phase separation. The largest values of χ for nonionic polymers reported to date are typically 0.1 (for PS−polybutadiene,[6] PS−P2VP [7]). We report a system with a value of χ at least an order of magnitude greater than these, which may be a candidate for experimental observation of the super-strong segregation regime.

The Flory−Huggins interaction parameter has been determined by a number of methods. Among the most common are small-angle light scattering[6] and neutron scattering.[8] However these methods require a degree of miscibility in the system, and therefore, it is not possible to use them for very strongly segregated polymers. In this case it is possible to obtain χ by measuring other parameters, such as the contact angle[9] and segregation isotherms.[10] Mean field theory provides expressions which relate the measured parameters to χ. We have used three such methods to obtain independent measurements of χ for the PS−P4VP system.

Method 1. Micelle Spacing in Microphase-Separated Diblocks

The microstructures formed by AB block copolymers, when the A and B blocks are incompatible, have been widely studied in recent years.[11,12] The microstructure is governed by the relative block lengths; for example, symmetric diblocks are known to form a lamellar phase in which each block forms a brush, where the junction points are confined to a narrow region. As the diblock becomes more asymmetric, the lamellae are replaced first by cylindrical and then spherical micelles (in some cases a bicontinuous phase also appears in a small region of the phase diagram).

The dependence of the micelle spacing and interfacial width on the properties of the polymers (such as

† Present address: Cavendish Laboratory, Madingley Road, Cambridge CB3 0HE, U.K.

⊗ Abstract published in *Advance ACS Abstracts,* June 1, 1997.

S0024-9297(96)01135-7 CCC: $14.00

molecular weight, segment length, and interaction parameter) is well understood in terms of mean field theory in the strong segregation limit. The principal results for the lamellar, cylindrical and spherical micelle spacings, h, are given by eqs 1, 2, and 3.[2,12] The

$$h_{\text{lamellar}} = 1.10aN^{1/2}(\chi N)^{1/6} \quad (1)$$

$$h_{\text{cylinder}} = \frac{2.06}{(1.645 - \ln f)^{1/3}} aN^{1/2}(\chi N)^{1/6} \quad (2)$$

$$h_{\text{sphere}} = \frac{1.78f^{1/3}}{(1 - 0.57f^{1/3})^{1/3}} aN^{1/2}(\chi N)^{1/6} \quad (3)$$

derivation assumes that the two polymers have similar statistical segment lengths, a (which is the case for PS and P4VP,[13] 6.7 Å). N is the total number of monomers in the diblock, and $f = N_A/(N_A + N_B) = N_A/N$ is the fraction of monomers of type A. By measuring the equilibrium micelle spacing for diblocks of PS and P4VP, it is possible to determine a value for χ. Four different PS−P4VP diblock copolymers were used, PS(200)-*b*-P4VP(200), PS(200)-*b*-P4VP(100), PS(260)-*b*-P4VP(71) and PS(130)-*b*-P4VP(15), where the numbers in parentheses are the polymerization numbers of each block. They were prepared by anionic polymerization and have narrow molecular weight distributions ($M_w/M_n < 1.1$). Thin films (approximately 1000 Å thick) were spin coated from DMF solution onto silicon wafers. Two different film thicknesses were used for each copolymer. The samples were annealed at 165 °C (for the 200−200 copolymer) and 180 °C (other copolymers) for 3 weeks. An ultra-high-vacuum oven was used to prevent degradation of the samples by oxidation during annealing. Samples were removed after 1, 2, and 3 weeks, and the surface topography was examined by atomic force microscopy (AFM), using a Digital Nanoscope III instrument in contact mode with a silicon nitride tip. It is known that if the thickness of the film is not an integral multiple of the equilibrium micelle spacing, islands and holes are formed on the surface, so that at any point on the film, the thickness is equal to an integral multiple of the spacing[14] (mh for the holes and $(m + 1)h$ for the islands, where m is an integer). This phenomenon has previously been observed for PS−P2VP diblocks with a cylindrical microstructure.[15] Thus when we see no further change in the surface topology, we can be certain that the sample has reached equilibrium.

Figure 1 shows atomic force micrographs of the surface topology of three samples (200−200, 200−100, and 260−71) which have been annealed for 3 weeks, from which we obtain the micelle spacing. The morphology of each sample was checked by transmission electron microscopy. Contrast was obtained by staining the P4VP regions with iodine. The 200−200 polymer was lamellar as expected. The 200−100 diblock, which lies close to the boundary between cylindrical and lamellar phases, showed cylindrical morphology, the 260−71 diblock was seen to contain a mixture of cylinders and spheres, and the 130−15 diblock had a spherical micelle morphology. Figure 2 shows transmission electron microscopy (TEM) images of the 200−100 cylinders and the 260−71 mixed morphology. The TEM of the 200−200 lamellar morphology is featureless and is not shown. A value for the micelle spacing for the 200−100 diblock can be directly obtained from the TEM images. However, this value must be treated with caution since the sample may swell when it is stained.

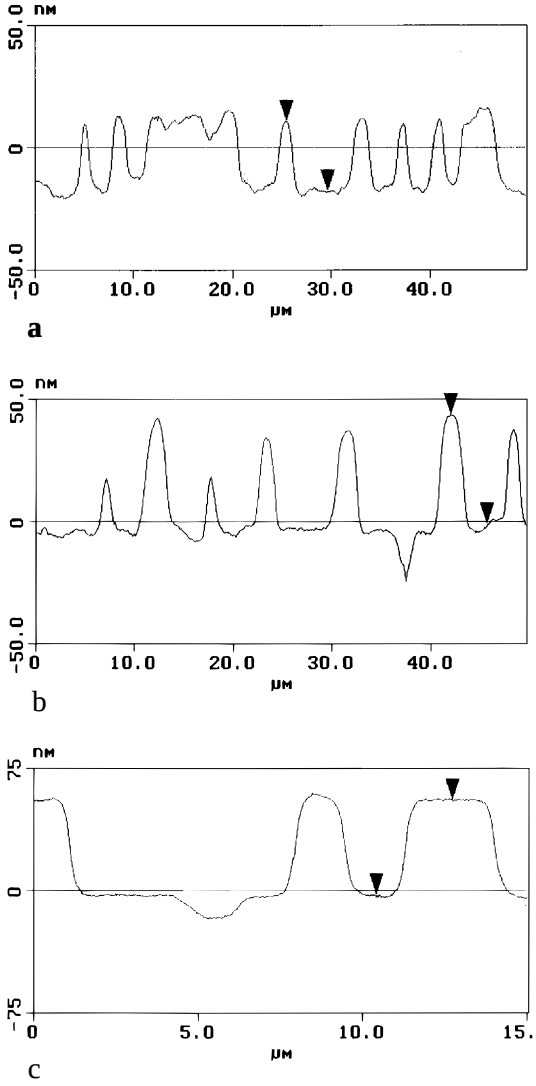

Figure 1. AFM cross-sections of the surface of PS−P4VP diblock films annealed for 3 weeks, showing islands and holes: (a) 260−71, (b) 200−100 and (c) 200−200. An image is also shown in a for the 260−71 diblock, which is typical of all the polymers.

We can also measure the micelle spacing with secondary ion mass spectrometry (SIMS). SIMS is a sensitive, direct depth profiling technique which has been extensively used to study polymer films.[16] It averages laterally over distances on the order 0.1 mm. We know from TEM that the morphology is laterally uniform, except for the 260−71 copolymer sample, so that this averaging does not affect our results. The mixed morphology of the 260−71 film makes it difficult to obtain χ reliably from the micelle spacing, so we do not calculate a value for that diblock. Figure 3 shows the P4VP volume fraction as a function of depth in the sample for the 200−100 copolymer film. This shows

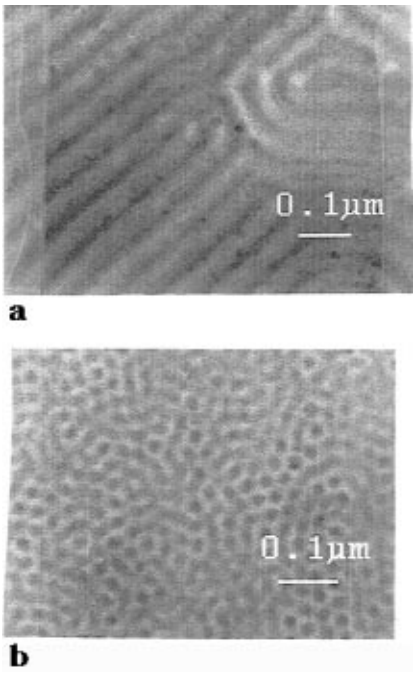

Figure 2. TEM images of diblock films: (a) 200−100, cylindrical morphology; (b) 260−71, mixture of cylinders and spheres. The dark regions are P4VP.

alternate layers of PS- and P4VP-rich regions (the volume fractions in these regions are not 0 and 1 because of the cylindrical morphology and the instrumental resolution). SIMS profiles for the other diblocks display similar layering. The depth scale is determined by the known total film thickness measured by ellipsometry and is linear because the sputtering rate is constant (i.e. independent of whether the material is PS or P4VP at any particular depth).

It is known that, close to a hard surface, the morphology may be different from the bulk. For example, a cylindrical bulk morphology becomes lamellar in the layer adjacent to a planar surface.[15] Our samples contain 4 or more layers, so when calculating the SIMS spacing, we discount the value for the layer next to the substrate. The spacings quoted are the mean values of the remaining layers.

The results of the SIMS, TEM, and AFM measurements are summarized in Table 1. The errors are calculated statistically for the AFM measurements (approximately 20 island and hole heights were measured for each diblock) and for SIMS, derived from the experimental uncertainty. The error in χ is relatively large because $\chi \sim h^6$. Errors in the other quantities in eqs 1−3 are small by comparison.

Method 2. Contact Angle

The contact angle that a liquid droplet makes on a substrate can be used to obtain the interfacial energy for the liquid at the substrate. The relationship between the contact angle and the interfacial energies was derived long ago by Young[17]

$$\gamma_{P4VP} = \gamma_{PS} \cos\theta + \gamma_{PS/P4VP} \qquad (4)$$

where γ_i are the surface tensions and θ is the equilibrium contact angle. Contact angle measurements of macroscopic droplets have been used for many years to study surfaces. Recently atomic force microscopy was used recently by Vitt and Shull to measure the contact angle of microscopic droplets of P2VP on PS[9] from which they obtained the surface energy of P2VP as a function

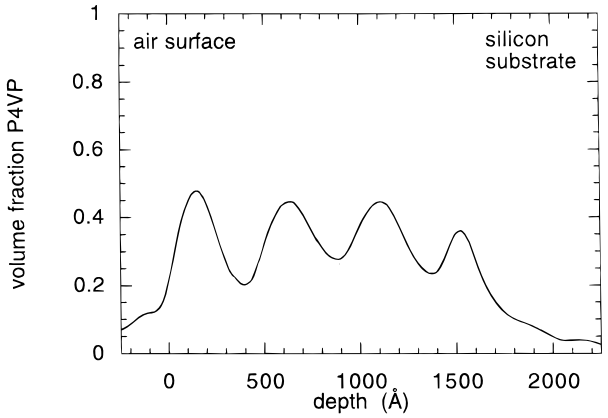

Figure 3. SIMS data showing the P4VP volume fraction as a function of depth for the 200−100 diblock.

of temperature. We measured the contact angle for droplets of PS on a thin film of P4VP, using a similar method. A layer of P4VP (M_w 50 000) 120 Å thick was spin coated onto a silicon wafer from solution in DMF. A layer of PS (M_w 50 000) 160 Å thick was spin coated onto a glass microscope slide and floated onto distilled water. It was picked up with the silicon wafer coated with P4VP to form a bilayer.

The sample was annealed at 183 °C for several days. Each day it was removed and examined by AFM. The PS film was observed to dewet and form droplets. After the sample was annealed for 7 days, most of the droplets were circular. Figure 4 shows an AFM image of a droplet. The contact angle can be measured by selecting two points on the surface of a droplet, one at the line of three-phase contact and the other a short distance away on the surface of the droplet. The contact angle is then calculated from the heights and horizontal separation of these points. However, it has been suggested that the detailed shape of the droplet in the vicinity of the contact line can be distorted by local forces.[19] In this case it is better to obtain the contact angle from the macroscopic height (H) and radius (R) of the droplet

$$\tan\left(\frac{\theta}{2}\right) = \frac{H}{R} \qquad (5)$$

for $\theta < 90°$. This requires only that the edge of the droplet is well defined so that R can be measured accurately. H and R were measured for several circular droplets. θ was observed to increase gradually on annealing, reaching a value of $(9.2 \pm 1.0)°$ after 7 days. This was obtained by averaging 20 different measurements.

If the lower (P4VP) layer were liquid, the dewetting drop could reduce its free energy by becoming lens shaped,[18] which would lead to an incorrect measurement of the contact angle. The P4VP layer was chosen to be very thin in our experiment so that the proximity of the PS droplet to the rigid substrate should ensure that it is flat on the bottom. This was checked by washing off the PS with toluene (a nonsolvent for P4VP) after the experiment had been completed. The remaining P4VP film was examined with AFM and found to be flat, confirming that the Young construction is appropriate.

The values are obtained in the glassy state, whereas the quantity we wish to measure is the contact angle of the melt polymers. Thus we must allow for the volume contraction of the PS on cooling from 183 °C to room temperature. This has been measured as 7−8% for PS.[20] We followed the procedure of Vitt and Shull[9]

Table 1. Micelle Spacings and Calculated χ for the Four Diblocks

polymer	temp (°C)	film thickness (Å)	AFM island eight (Å)	SIMS micelle spacing (Å)	χ
200−200	165	830	600 ± 40	540 ± 30	7.5 (+3, −2)
200−200	165	1034		560 ± 30	
200−100	180	1255	430 ± 40	460 ± 30	3.5 (+1.5, −1.0)
200−100	180	1780	535 ± 50 (TEM)	475 ± 40	
260−71	180	990	325 ± 55	360 ± 35	
260−71	180	1435		320 ± 40	
130−15	180	1435	180 ± 20		1.4 (+1.1, −0.7)

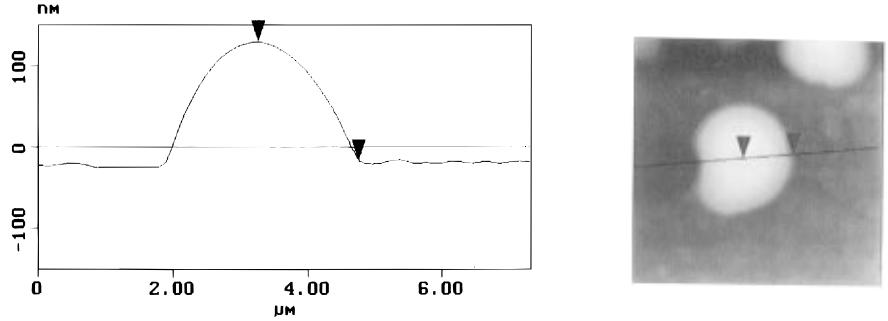

Figure 4. AFM image and cross section of a PS droplet on a layer of P4VP, from which the contact angle is measured.

when correcting our data for this effect. Using this method we obtain an equilibrium contact angle of (10.9 ± 1.0)°. We can calculate the surface energy for PS/P4VP from Young's equation. The surface energy of PS at 183 °C is 29.1 mN m^{-1}.[21] We are not aware of any measurements of the surface tension of P4VP in the literature. However the surface energy of P2VP has been measured as 35 mN m^{-1} at 183 °C.[9,22] We attempted to measure the surface tension of P4VP (by a modified Wilhelmy method), but this was impossible because the available homopolymer was too viscous. We would expect the value to be no less than, and possibly somewhat larger than, P2VP.[22] Using the P2VP value, we obtain an interfacial energy of 6.4 mN m^{-1} for PS/P4VP.

Helfand and Tagami[4] used mean field theory to relate the interfacial tension to χ

$$\gamma = a\rho k_B T\left(\frac{\chi}{6}\right)^{1/2} \quad (6)$$

where $1/\rho$ is the monomer volume. From this we obtain $\chi = 0.38$. It should be noted however that a 10% increase in the value used for the surface tension of P4VP increases χ by a factor of 2.4. Thus, since we have only estimated the surface tension of P4VP from the value for P2VP, we should not consider this result to be very precise. It seems unlikely that the surface tension of P4VP is less than 35 mN m^{-1}, so we consider that from the contact angle measurement we can only obtain a lower limit for χ.

Method 3. Interfacial Width

The width (a_I) of the interfacial region between two immiscible homopolymers is determined by a balance of enthalpic and entropic terms: a sharp interfacial width results in a loss of configurational entropy while a broad one introduces unfavorable interactions between unlike monomers. In the limit of high molecular weight, and where the polymers have similar step lengths[4]

$$a_I = 2a/(6\chi)^{1/2} \quad (7)$$

Small corrections to this arise when the polymers have different step lengths[23] and arise for finite molecular weights.[24]

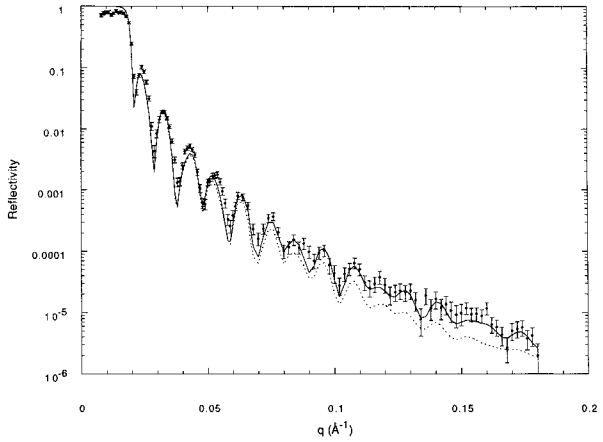

Figure 5. Reflectivity data (symbols) and best fit simulation (solid line) for the PS−P4VP bilayer. The dashed line shows a simulation with a width of 10 Å.

Neutron reflectometry is a powerful tool for investigating surface and interface phenomena in thin polymer films[25] because of its sensitivity and resolution. It has been used by several groups to determine interfacial widths between immiscible polymers.[5,26−28] A bilayer sample was prepared on a 3 in. diameter silicon wafer. The bottom layer of dPS (M_w = 713K; thickness = 562 Å) was spin coated onto a silicon wafer. A layer of P4VP (M_w 100K; thickness 400 Å) was spin coated onto glass and floated onto the surface of a bath of distilled water. This was then picked up on top of the PS-coated silicon wafer and annealed for 2 h at 160 °C under vacuum. The reflectivity experiment was performed on the H9A′ reflectometer at the High Flux Beam Reactor at Brookhaven National Laboratory. Figure 5 shows the reflectivity data (symbols) and best fit, obtained using the known layer thicknesses (solid line). The roughness at the air surface was measured for similar samples by X-ray reflectivity, and a value of 5 Å is typical. This was assumed when fitting the reflectivity data, although since the top layer is the P4VP (low neutron scattering length density) it does not have a large effect on the fit.

When interfacial widths measured by neutron reflectometry are compared with the prediction from mean field theory, it is necessary to account for capillary wave fluctuations in the position of the interface. These fluctuations, which are averaged by the reflectivity

Table 2. Summary of the Measurements of χ

technique	polymer	temp (°C)	χ	error
micelle spacing (SIMS, AFM)	200−200	165	7.5	+3.0, −2.0
micelle spacing (SIMS, AFM, TEM)	200−100	180	3.5	+1.5, −1.0
micelle spacing (AFM)	130−15	180	1.4	+ 1.1, −0.7
contact angle (AFM)	homopolymers	183	0.4	lower limit
interface width (NR)	homopolymers	160	1.0	lower limit

experiment, cause the measured interfacial width to be larger than the intrinsic width. The measured width is the convolution of the two contributions (intrinsic width and capillary waves). We can calculate the expected contribution of the capillary waves if the interfacial tension is known. The mean square displacement of the interface from its average position due to capillary waves, $\langle(\Delta z)^2\rangle$ is[29,30]

$$\langle(\Delta z)^2\rangle = \frac{k_B T}{2\pi\gamma}\ln\left(\frac{\lambda_{max}}{\lambda_{min}}\right) \quad (8)$$

The cutoff wavelengths, λ_{min} and λ_{max}, are the shortest and longest wavelength fluctuations which contribute to the measured interfacial widths. The upper limit is given by the in plane coherence length of the neutrons in the experiment (~10 000 Å on H9A′) and the lower is usually estimated as the intrinsic interfacial width (we use 5 Å). However because of the logarithmic dependence on these wavelengths, the choice of these values is not crucial. This expression has been used previously to estimate the capillary wave contribution to the measured interfacial width from NR experiments on immiscible homopolymer bilayers and was found to account for the discrepancy between the measured width and the mean field prediction.[29]

From eqs 7 and 8, we obtain the measured interfacial width in terms of χ.

$$w = \left[\frac{4a^2}{6\chi} + \frac{1}{2\pi a\rho}\sqrt{\frac{6}{\chi}}\ln\left(\frac{\lambda_{max}}{\lambda_{min}}\right)\right]^{1/2} \quad (9)$$

The interface was modeled with a hyperbolic tangent profile for which the only unknown quantity is the interfacial width. As this is increased from 0 to 7 Å, the quality of the fit to the data (measured by the least-squares parameter) changes little. This reflects the fact that we are at the limit of resolution of the reflectivity technique. Above 7 Å the fit quality becomes worse. We conclude that the interface width is less than 10 Å because above this value χ^2 increases significantly.[31] The fit for a 10 Å interfacial width is shown as the dashed line in Figure 5. From eq 9, a measured width of 10 Å gives $\chi \approx 1.0$. We note that there are several possible inaccuracies in this approach. First, eq 8 does not necessarily account for all contributions to the roughness at the interface; for example the film may become buckled as a result of the floating process, which could also trap water, or other impurities, at the interface. However these contributions would increase the measured interfacial width, and this would lead to an overestimate of the intrinsic width. In addition, the accuracy of the mean field expression for the intrinsic interfacial width may be questionable for widths smaller than a monomer size. Therefore we cannot use this method to obtain an exact value of χ, but we may obtain an upper limit on the interface width and therefore a lower limit on χ of 1.0.

Conclusion

Table 2 summarizes the measurements of χ from all the experiments. We conclude that the value of the Flory−Huggins interaction parameter for PS/P4VP blends is very large. We obtain values of 7.5, 3.5 and 1.4, and >1.0. Thus, although we are not able to obtain a precise value, even the lower limit is an order of magnitude greater than the largest values of χ reported in other nonionic systems. It is likely that χ is temperature and/or composition dependent, and this may partially account for the variation in our measurements. It is also possible that the use of the strong segregation mean field theory is not valid, as we approach the super-strong regime. The large value of χ makes the PS/P4VP system a candidate for experimental observations of this regime.

Acknowledgment. This work was in part supported by the following grants: NSF DMR 9316157, DOE FG0293ER45481, and NSERC CPG0163892.

References and Notes

(1) Leibler, L. *Macromolecules* **1980**, *13*, 1602.
(2) Semenov, A. N. *Sov. Phys. JETP* **1985,** *61*, 733; *Macromolecules* **1992**, *25*, 4967.
(3) Nyrkova, I. A.; Khokhlov, A. R.; Doi, M. *Macromolecules* **1993**, *26*, 3601. Semenov, A. N.; Nyrkova, I. A.; Khokhlov, A. R. *Macromolecules* **1995**, *28*, 7491.
(4) Helfand, E.; Tagami, Y. *Polym. Lett.* **1971**, *9*, 741; *J. Chem. Phys.* **1971**, *56*, 3592.
(5) Anastasiadis, S. H.; Russell, T. P.; Satija, S. K.; Majkrzak, C. F. *Phys. Rev. Lett.* **1989**, *62*, 1852.
(6) Roe, R.-J.; Zin, W.-C. *Macromolecules* **1980**, *13*, 1221.
(7) Shull, K. R.; Kramer, E. J.; Hadziioannou, G.; Tang, W. *Macromolecules* **1990**, *23*, 4780.
(8) Bates, F. S.; Wignall, G. D. *Phys. Rev. Lett.* **1986**, *57*, 1429.
(9) Vitt, E.; Shull, K. R. *Macromolecules* **1995**, *28*, 6349.
(10) Dai, K. H.; Kramer, E. J. *Polymer* **1994**, *35*, 157.
(11) Bates, F. S.; Fredrickson, G. H. *Annu. Rev. Phys. Chem.* **1990**, *41*, 525.
(12) Rubinstein, M.; Obukhov, S. P. *Macromolecules* **1993**, *26*, 1740.
(13) Dai, K. H.; Norton, L. J.; Kramer, E. J. *Macromolecules* **1994**, *27*, 1949.
(14) Coulon, G.; Collin, B.; Auserre, D.; Chatenay, D.; Russell, T. P. *J. Phys. (Paris)* **1990**, *51*, 2801. Coulon, G.; Auserre, D.; Russell, T. P. *J. Phys. (Paris))* **1990**, *51*, 777.
(15) Liu, Y.; *et al. Macromolecules* **1994**, *27*, 4000.
(16) Schwarz, S. A.; *et al. Mol. Phys.* **1992**, *76*, 937.
(17) Young, T. *Phil. Trans. Roy. Soc. London* **1805**, *5*, 65.
(18) Brochard Wyart, F.; Martin, P.; Redon, C. *Langmuir* **1993**, *9*, 3682.
(19) Leibler, L.; Ajdari, A.; Mourran, A.; Coulon, G.; Chatenay, D. In *Ordering in Macromolecular Systems*, Teramoto, A., Norisuje, M. K. T., Eds.; Springer-Verlag: Berlin, 1994.
(20) Hellwege, K. H.; Knappe,W.; Lehmann, P. *Kolloid Z.* **1963**, *183*, 110.
(21) Dee, G. T.; Sauer, B. B. *J. Colloid Interface Sci.* **1992**, *152*, 85.
(22) Sauer, B. B. *Private communication.*
(23) Helfand, E.; Sapse, A. M. *J. Chem. Phys.* **1975**, *62*, 1327.
(24) Broseta, D.; Fredrickson, G. H.; Helfand, E.; Leibler, L. *Macromolecules* **1990**, *23*, 132.
(25) Russell, T. P. *Mater. Sci. Rep.* **1990**, *5*, 171.
(26) Fernandez, M. L.; Higgins, J. S.; Penfold, J.; Ward, R. C.; Shackleton, C.; Walsh, D. J. *Polymer* **1988**, *29*, 1923.
(27) Genzer, J.; Composto, R. J. *Bull. Am. Phys. Soc.* **1993**, *38*, 488.
(28) Clarke, C. J.; Jones, R. A. L.; Edwards, J. L.; Shull, K. R.; Penfold, J. *Macromolecules* **1995**, *28*, 2042.
(29) Shull, K. R.; Mayes, A. M.; Russell, T. P. *Macromolecules* **1993**, *26*, 3929.
(30) Semenov, A. N. *Macromolecules* **1993**, *26*, 6617.
(31) At 10 Å, the value of the normalized least-squares fit parameter has increased by one over its minimum value. Thus we can consider 10 Å as an upper limit for the measured interface width.

MA961135L